

## Mass segregation of embedded clusters in the Milky Way \*

Xin-Yue Er<sup>1,2</sup>, Zhi-Bo Jiang<sup>1</sup> and Yan-Ning Fu<sup>1</sup>

<sup>1</sup> Purple Mountain Observatory, Chinese Academy of Sciences, Nanjing 210008, China;  
[xy@pmo.ac.cn](mailto:xy@pmo.ac.cn)

<sup>2</sup> Graduate University of Chinese Academy of Sciences, Beijing 100049, China

Received 2012 September 12; accepted 2012 October 18

**Abstract** Embedded clusters are ideal laboratories for understanding the early phase of the dynamical evolution of clusters as well as massive star formation. An interesting observational phenomenon is that some of the embedded clusters show mass segregation, i.e., the most massive stars are preferentially found near the cluster center. We develop a new approach to describe mass segregation. Using this approach and the Two Micron All Sky Survey Point Source Catalog (2MASS PSC), we analyze 18 embedded clusters in the Galaxy. We find that 11 of them are mass-segregated and that the others are not mass-segregated. No inversely mass-segregated cluster is found.

**Key words:** open clusters and associations: general — stars: formation — methods: data analysis

### 1 INTRODUCTION

In recent years, the development of near infrared instruments has deepened our knowledge of embedded clusters in the Galaxy. Some of the embedded clusters show mass segregation, i.e., the most massive stars are preferentially found near the cluster center. This phenomenon has been observed in the Trapezium (Hillenbrand 1997; Hillenbrand & Hartmann 1998), NGC 6611 (Bonatto et al. 2006), M17 (Jiang et al. 2002), NGC 1333 (Lada et al. 1996), NGC 2244 and NGC 6530 (Chen et al. 2007). More details on this topic can be found in the reviews (Elmegreen et al. 2000; Lada & Lada 2003).

Mass segregation of embedded clusters can be dynamical. McMillan et al. (2007) find that mass-segregated clusters can be quickly formed by merging several subclusters. Simulations by Allison et al. (2009b) and Yu et al. (2011) confirm that the violent evolution of a cool, fractal cluster can give rise to mass segregation in a short timescale ( $\sim 1$  Myr).

Mass segregation of embedded clusters can also be primordial. According to Jeans theory, Jeans mass tends to be smaller, thus yielding less massive protostars, due to higher density in the center of a molecular core than that in the outskirts, whereas these protostars will accumulate gas and eventually evolve into massive stars more easily through competitive accretion (Larson 1982; Murray & Lin 1996; Bonnell et al. 1997). In addition to the mechanism of competitive accretion, it is argued that the protostars are so rich in the cluster center that they can merge into the massive stars (Bonnell et al. 1998; Bonnell & Bate 2005).

---

\* Supported by the National Natural Science Foundation of China.

Moreover, mass segregation of embedded clusters may not be “true.” For instance, Ascenso et al. (2009) argue that it might be an observational bias in some cases. Er et al. (2009) argue that it might be a temporary aggregation resulting from the random motions of massive stars.

It can be seen that studying mass segregation of embedded clusters will help us in understanding the early dynamical evolution of clusters and massive star formation. However, so far it has not been clear whether or not mass segregation is a common phenomenon associated with embedded clusters. Consequently, we analyze the mass segregation of 18 clusters in our Galaxy in this paper. In Section 2, we describe our approach based on a new index— $\mathcal{R}$ . In Section 3, with realistic clusters, we show the validity of the approach. In Section 4, we analyze the status of the mass segregation of 18 clusters. In Section 5, we discuss the implications of our results. In Section 6, a summary is given.

## 2 DESCRIPTION OF MASS SEGREGATION

### 2.1 A Brief Review

Hillenbrand (1997) uses the variation of the ratio of massive stars to low-mass stars in different regions to probe mass segregation. Mass segregation can also be reflected in the variations of mean stellar mass (Hillenbrand & Hartmann 1998), mass function, and luminosity function (Hunter et al. 1995; Brandl et al. 1996; Vázquez et al. 1996; Fischer et al. 1998; de Grijs et al. 2002; Kerber & Santiago 2006). Nevertheless, as pointed out by Gouliermis et al. (2004) and Apellániz & Úbeda (2005), one should note the uncertainty caused by the determination of the slope of power laws.

From another viewpoint, the distribution of massive stars is more concentrated than that of low-mass stars in a mass-segregated cluster. This will lead to the half-number radius of the massive stars being smaller than that of low-mass stars (Zhao et al. 2006). Also, the surface number density profiles of massive stars and low-mass stars are different (Lada et al. 1991). If profiles are characterized by a power-law, the indices are different (Sagar et al. 1988; Kontizas et al. 1998); if profiles are characterized by the King model (King 1962, 1966), the core radii are different (Nürnberger & Petrotzakis 2002). Moreover, the profiles can be characterized by different models. For M17, Jiang et al. (2002) find an exponential radial decline for massive stars and a power-law radial decline for low-mass stars. Sometimes the profiles are transformed into cumulative forms in which their differences are checked by the Kolmogorov-Smirnov test (Zhao et al. 2006; Chen et al. 2007). Actually, the Kolmogorov-Smirnov test can be directly applied to the distributions of massive stars and low-mass stars (Hillenbrand & Hartmann 1998; Raboud & Mermilliod 1998).

Recently, Allison et al. (2009a) introduced  $\Lambda$ , the ratio of the length of the minimum spanning tree of massive stars to that of low-mass stars, to characterize mass segregation. The advantage of this index is that it does not rely on defining the cluster center. In the present work, we develop a new approach to describe mass segregation.

### 2.2 A New Index

We define the new index as  $\mathcal{R} = \frac{\bar{L}_{\text{part}}}{\bar{L}_{\text{all}}}$ , where  $\bar{L}_{\text{part}}$  is the mean mutual distance of a special class of stars, and  $\bar{L}_{\text{all}}$  that of all stars. If  $\mathcal{R} < 1$ , the distribution of the special class of stars is more concentrated. The smaller  $\mathcal{R}$  is, the more pronounced the concentration. When the special class of stars refers to most massive stars,  $\mathcal{R}$  becomes an index of mass segregation.

Note that the deviation of  $\mathcal{R}$  from unity does not necessarily mean mass segregation, for it can be merely a consequence of fluctuation. In order to cope with the fluctuation, numerical tests have been performed to obtain a reasonable threshold of  $\mathcal{R}$ . We generate 100 cluster samples, each consisting of 1000 stars with different masses (Cartwright & Whitworth 2004). The stars are distributed independently of mass following a surface number density profile in the form of  $\rho \propto r^{-1}$ , where  $r$  is the radial distance. Provided that the number of top most massive stars ( $N_{\text{top}}$ ) is fixed,  $\mathcal{R}$  can be

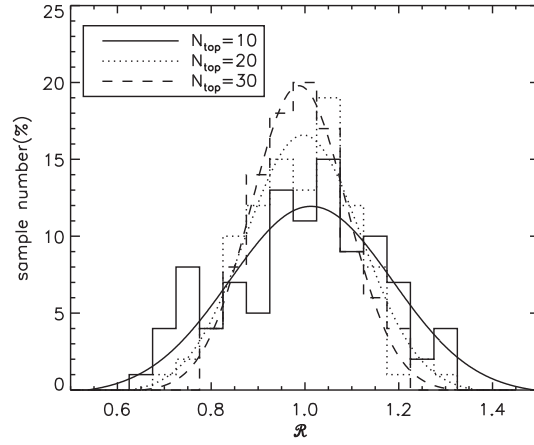


**Fig. 1** Histograms of  $\mathcal{R}$  for 100 artificial cluster samples. We fit the values of  $\mathcal{R}$  by Gaussian distributions.

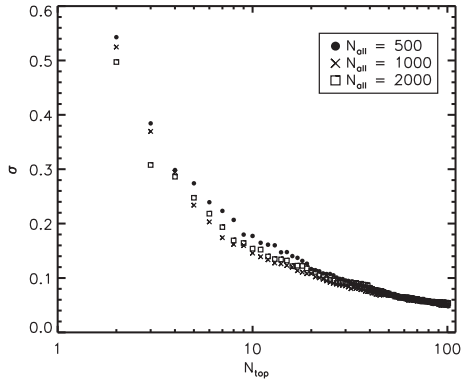


**Fig. 2** The dependences of  $\sigma$  on  $N_{\text{top}}$  and  $N_{\text{all}}$ .

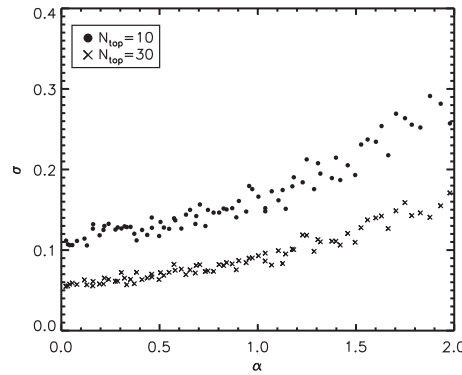


**Fig. 3** The dependence of  $\sigma$  on  $\alpha$ .

well fitted by a Gaussian distribution within the confidence interval of  $3\sigma$ , where  $\sigma$  is the standard deviation (see Fig. 1). Following the definition of the Gaussian distribution, the samples far smaller than unity can be regarded as being mass segregated. In other words, we can obtain the threshold of  $\mathcal{R}$  from  $\sigma$ . Further tests suggest that  $\sigma$  is related to  $N_{\text{top}}$ , since the width of the Gaussian curve becomes narrower as  $N_{\text{top}}$  increases from 10 to 30.

Figure 2 shows  $\sigma$  is a function of  $N_{\text{top}}$ . When  $N_{\text{top}}$  is small,  $\sigma$  is extremely large and declines rapidly with the increase of  $N_{\text{top}}$ . For larger  $N_{\text{top}}$ , the change of  $\sigma$  becomes smaller. This suggests that the dependence of  $\sigma$  on  $N_{\text{top}}$  should be taken into account. Indeed, this also illustrates that mass segregations deduced from only a few stars are inherently uncertain, as Lada & Lada (2003) argued. We also generate two other sets of cluster samples in which the numbers of cluster members ( $N_{\text{all}}$ ) are 500 and 2000. Their dependences of  $\sigma$  on  $N_{\text{top}}$  are obtained and presented in Figure 2. It can be seen that the effect of  $N_{\text{all}}$  is much weaker than that of  $N_{\text{top}}$ . Thus, we do not consider its effect in this paper. The number density profiles of realistic clusters are generally different. They can be roughly represented by the form of  $\rho \propto r^{-\alpha}$ . Figure 3 shows that  $\sigma$  grows with an increasing  $\alpha$ . This suggests that the effect on  $\sigma$  due to the profiles should be considered.

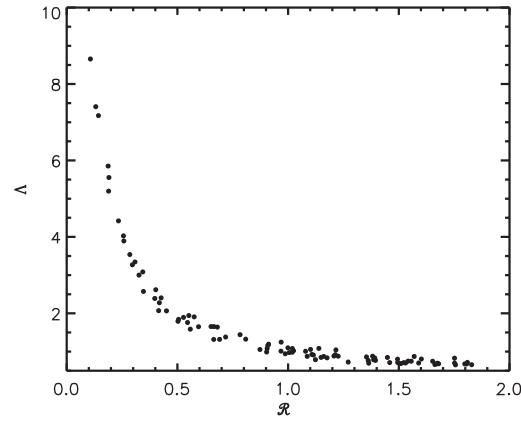


**Fig. 4** Comparison between  $\mathcal{R}$  and  $\Lambda$ .

For a given cluster of 1000 stars, we select ten stars as a set and calculate its  $\mathcal{R}$  and  $\Lambda$ . In order to study their relations in different environments, we select many sets in which stars are distributed at different degrees of concentration. Figure 4 shows that they have a good correlation, which indicates that  $\mathcal{R}$  is another choice for describing mass segregation. It is worth mentioning that the time consumed for calculation of  $\mathcal{R}$  is  $\propto N$ , while that of  $\Lambda$  is  $\propto N^2$ .

### 2.3 $\mathcal{R} - N_{\text{top}}$ Plot

Obviously, the  $\mathcal{R}$  value of a cluster depends on the chosen  $N_{\text{top}}$ . So an  $\mathcal{R} - N_{\text{top}}$  plot is introduced to describe the status of the mass segregation of a cluster. Figure 5 shows the  $\mathcal{R} - N_{\text{top}}$  plots of four typical artificial clusters.

Panel (a) shows the case of a non-mass-segregated cluster. The stars in the cluster are distributed independently of mass. Although some of the  $\mathcal{R}$  are lower than unity, few of them are lower than unity with  $1\sigma$  confidence. This kind of deviation of  $\mathcal{R}$  from unity can be viewed as a fluctuation. Panel (b) shows the case of general mass segregation. In this cluster we place the top five percent of stars inside the half number radius of the cluster. We find nearly all the values of  $\mathcal{R}$  are lower than unity and most of them are lower than unity with  $1\sigma$  confidence. Panel (c) shows the case of dynamical mass segregation. In this cluster, the radial distance of each star is strictly related to its mass, with the most massive stars located innermost and the lowest-mass stars outermost. As is shown,  $\mathcal{R}$  has a smooth increase in a wide mass range. Panel (d) shows the case of primordial mass segregation. In this cluster, the top five most massive stars are in the center region and the other stars are distributed independently of mass. One may find an abrupt increment of  $\mathcal{R}$  at  $N_{\text{top}} = 5$ . Although we only rearrange the top five most massive stars, the effect seems to exist until  $N_{\text{top}} \sim 100$ . This is because these five massive stars are located in the very center of the cluster, and  $\mathcal{R}$  at  $N_{\text{top}} = 100$  contains all the position information from  $N_{\text{top}} = 2$  to 100.

### 2.4 Definition of Mass Segregation for a Cluster

The primary goal of this paper is to study whether or not mass segregation is a common phenomenon for embedded clusters. Therefore we set a definition to classify clusters into two categories, i.e., with or without mass segregation, ignoring the details of the  $\mathcal{R} - N_{\text{top}}$  plot. Considering that the dispersion of  $\mathcal{R}$  is especially large for small  $N_{\text{top}}$ , we restrict ourselves to  $5 \leq N_{\text{top}} \leq N_{\text{all}}$ . In this range we try to find the largest number of  $N_{\text{top}}$ , denoted as  $N_x$ , such that the values of  $\mathcal{R}$  from  $N_{\text{top}}$

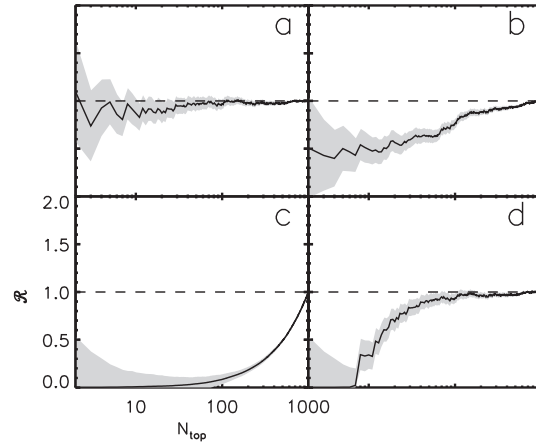


**Fig. 5**  $\mathcal{R} - N_{\text{top}}$  plot of four typical artificial clusters. The gray shaded band shows the  $1\sigma$  level confidence region of mass segregation. Panel (a) is a non-mass-segregated cluster. Panel (b) is a general mass-segregated cluster. Panel (c) is the case of dynamical mass segregation. Panel (d) is the case of primordial mass segregation.

$= 5$  to  $N_x$  satisfy: (1) They are all lower than unity. (2) Half of them are lower than  $1 - s \times \sigma$ , where  $s$  is called the level of mass segregation. In this paper, we choose  $s = 1$  or  $3$ .

If  $N_x$  exists for a given  $s$ , we consider the cluster to be level- $s$  mass-segregated in the range from  $N_{\text{top}} = 5$  to  $N_x$ ; if  $N_x$  does not exist, we consider the cluster to be non-mass-segregated. We believe that this quantitative definition can distinguish between fluctuation and real mass segregation.

### 3 TEST OF VALIDITY FOR OUR APPROACH

#### 3.1 Sampling a Cluster

The positional and photometric data of the clusters are extracted from 2MASS PSC in  $Ks$  band. In order to guarantee the reliability, the following data are excluded from consideration.

- (1) “Kmag > 14.3 mag,” since 14.3 mag is the limiting magnitude of the  $Ks$  band. Most of the discarded stars are due to this reason.
- (2) “Qflg = U,” which means the catalog only gives the upper limit on magnitude.
- (3) “use = 0,” which means the source is an apparition.
- (4) “Xflg = 0” and “extkey is null,” which means the source is an extragalactic source.
- (5) “Aflg = 1,” which means the source is associated with a known solar system object.
- (6) “Qflg = X,” which means there is no valid brightness measurement, although a detection is found.

The top panel of Figure 6 shows the surface density map of the Orion Nebula Cluster (ONC) in a  $30' \times 30'$  field. Assuming that the most populated area is the cluster center, we construct its radial density profile in the bottom panel of Figure 6. The uniform model  $\rho(r) = \frac{C_0}{r^{C_1}} + C_2$  is used as a fitting model for the profile, where  $C_0$  is a fitting parameter,  $C_1$  is the index of the profile, and  $C_2$  stands for the surface number density of background stars. We truncate the cluster at the radius where  $\rho(r) = 3C_2$ . There are cases in which the best fitting value of  $C_2$  is negative. To avoid this and to be consistent in processing all sample clusters, we do not adjust  $C_2$  in the fitting. Instead, we

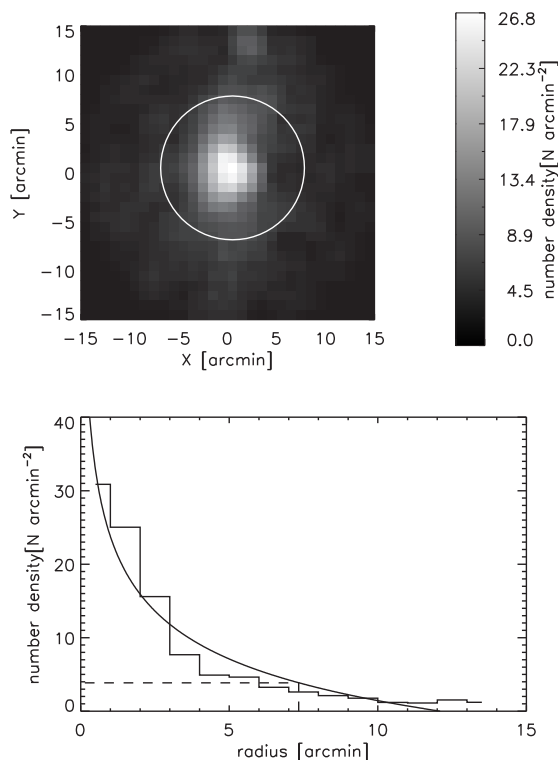


**Fig. 6** Surface density map of ONC (*top*) and its surface number density profile (*bottom*). The circle (*top*) and dashed line (*bottom*) show the radius we determine.

fix its value roughly as the mean density of the background. All the clusters considered in this paper are truncated in the same way as above.

Identification of members of a cluster is rather difficult. Anderson & King (2003), Chen et al. (2007) and Pang et al. (2010) use proper motion to identify the memberships. However, this method needs a long term observation that spans many years. Soares & Bica (2002) and Bonatto & Bica (2003; 2005) use color-magnitude and color-color diagrams to identify the memberships. However, this method still contains uncertainties from the photometry and the evolutionary track. Because of the facts that the associated clouds give rise to severe extinction of embedded clusters and that our cluster samples are all closer than 2kpc, we estimate that the background and foreground stars within the truncated radius of a cluster are less than 10%. That is, the effect of contamination is statistically insignificant. As a result, we regard all the stars in the truncated radius as being cluster members.

### 3.2 Case of ONC

ONC is the most famous star formation region with a mean age of less than 1 Myr (Hillenbrand 1997). The cluster shows apparent mass segregation (Hillenbrand 1997; Hillenbrand & Hartmann 1998). We take it as an example to show the validity of our approach. Figure 7 shows the  $\mathcal{R} - N_{\text{top}}$  plot of ONC. Generally speaking,  $\mathcal{R}$  has an increasing trend with  $N_{\text{top}}$ , although the trend is non-monotonic. Following our definition, ONC is mass-segregated. In fact, the mass segregation is so pronounced that ONC can be viewed as a level-3 mass-segregated cluster.

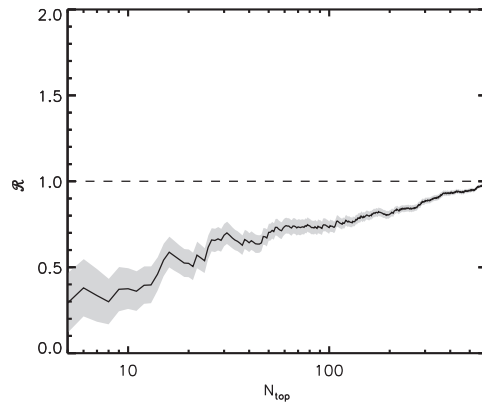


**Fig. 7** The  $\mathcal{R} - N_{\text{top}}$  plot of ONC. Symbols denote the same as in Fig. 5.

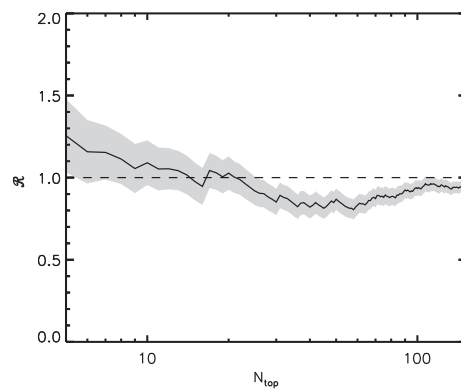


**Fig. 8** The  $\mathcal{R} - N_{\text{top}}$  plot of Mon R2. Symbols denote the same as in Fig. 5.

Allison et al. (2009a) also consider that ONC is mass-segregated, whereas they argue that ONC is only mass-segregated for the top ten most massive stars. This inconsistency results from the different cluster members which are used. Specifically, our cluster's center is in agreement with theirs, but our cluster's extent is about half of theirs. Moreover, significantly more dim stars are detected by 2MASS in this region. Notice that Allison et al (2009a) argue their data set may lack low-mass stars, since they only use the stars that are provided with masses.

### 3.3 Case of Mon R2

Mon R2 is another embedded cluster close to us. As is shown in Figure 8, its  $\mathcal{R} - N_{\text{top}}$  plot is quite different from that of ONC.  $\mathcal{R}$  is slightly larger than unity at the beginning, then falls until  $N_{\text{top}} \sim 60$ , and then rises again.  $\mathcal{R}$  is lower than  $1 - \sigma$  from  $N_{\text{top}} \sim 30$  to 100. These facts indicate that the distribution of the most massive stars is more scattered than that of all stars, but quite a few intermediate mass stars are distributed in the center region. Following our definition, Mon R2 is non-mass-segregated. Carpenter et al. (1997) also consider that Mon R2 does not present compelling evidence of mass segregation.

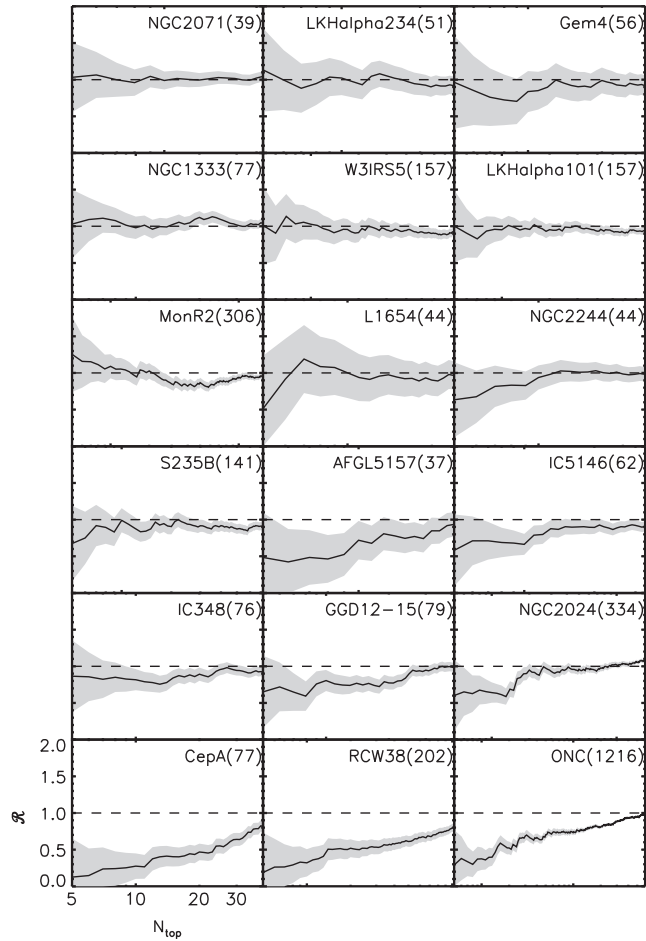


**Fig. 9** The  $\beta - N_{\text{top}}$  plots of 18 embedded clusters. The cluster's name and number of stars are marked in the top right corner of each panel. The gray shaded band shows the  $1\sigma$  level confidence region of mass segregation.

## 4 RESULTS

Our embedded cluster samples come from the catalog of Lada & Lada (2003). However, using the method described in Section 3, we only identify 18 clusters from their catalog. Notice that we require that the cluster's density is three times more than that of the background. So the clusters that have a high contamination surrounding the cluster fail to be identified. Likewise, some clusters are excluded from consideration due to their scarcity of cluster members. Lada & Lada (2003) argue that 35 stars can make the cluster survive evaporation during its lifetime, so the clusters in their catalog have more than 35 cluster members. But the short exposure time of 2MASS PSC and different adopted cluster radii cause some of the clusters to have less than 35 members in our analysis. Considering that a sufficient number of stars is also necessary for statistical significance, these clusters are not taken into account in this paper. It is worth mentioning that, in order to enrich our cluster samples, we have tried other embedded cluster catalogs (Dutra et al. 2001; Dutra et al. 2003), but no new sample was found.

**Table 1** The Catalog of 18 Embedded Clusters

EC	Name	R.A. (J2000) (h m s)	Dec. (J2000) (° ' ")	Distance (pc)	Radius (pc)	$N_{\text{all}}$	Mass segregation status	Mass segregation range ( $N_x$ )
1	NGC 2071	05 47 08.0	+00 20 49	400	0.26	39	N	–
2	LkHalpaha 234	21 43 00.0	+66 06 59	1000	0.43	51	N	–
3	Gem 4	06 08 43.0	+21 31 19	1500	0.53	56	N	–
4	NGC 1333	03 29 04.0	+31 21 24	318	0.40	77	N	–
5	W3 IRS 5	02 25 39.0	+62 06 22	2400	1.35	157	N	–
6	LkHalpaha 101	04 30 12.0	+35 16 55	800	0.90	157	N	–
7	Mon R2	06 07 45.0	–06 23 29	800	0.97	306	N	–
8	L1654	06 59 44.0	–07 46 59	1100	0.32	44	Y	5
9	NGC 2244	06 34 13.0	+04 26 43	1600	0.64	44	Y	11
10	S235B	05 40 55.0	+35 40 55	1800	1.28	141	Y	15
11	AFGL 5157	05 37 46.0	+31 59 54	1800	0.56	37	Y	25
12	IC 5146	21 53 27.0	+47 15 31	1200	0.48	62	Y	41
13	IC 348	03 44 36.0	+32 08 46	320	0.23	76	Y	63
14	GGD 12-15	06 10 49.0	–06 12 24	800	0.58	79	Y	59
15	NGC 2024	05 41 45.0	–01 55 00	400	0.57	334	Y	71
16	CepA	22 56 21.0	+62 02 27	700	0.27	77	Y	66
17	RCW 38	08 59 03.0	–47 30 12	1700	0.73	202	Y	202
18	ONC	05 35 19.0	–05 22 44	450	0.96	1216	Y	682

The  $\mathcal{R} - N_{\text{top}}$  plots of the 18 clusters are presented in Figure 9. Table 1 lists their name, location, distance, radius, number of members, status of mass segregation, and mass segregation range. For NGC 2071, LkHalpaha 234, Gem 4, NGC 1333, W3 IRS 5, and LkHalpaha 101, all the  $\mathcal{R}$  are close to unity, so they are non-mass-segregated. Mon R2 also belongs to this category. L1654, NGC 2244, S235B, AFGL 5157, IC 5146, IC 348, and GGD12-15 are level-1 mass-segregated in a certain range (see the details in Table 1). Mass segregation of NGC 2024, CepA, and RCW 38 are rather pronounced. They are all level-3 mass-segregated in a certain range (from  $N_{\text{top}}=5$  to 15, 65, and 202). ONC also belongs to this category.

In conclusion, according to our definition, 11 clusters are level-1 mass-segregated, among which four clusters (NGC 2024, CepA, RCW 38, and ONC) are level-3 mass-segregated. The other clusters are non-mass-segregated. No cluster is found with convincing evidence for inverse mass segregation.

## 5 DISCUSSION

### 5.1 Variation of Parameter in Data Processing

The limiting magnitude of unconfused regions of 2MASS is 14.3 mag for Ks band. However, for the crowded cluster center, the limiting magnitude might be less than 14.3 mag. Therefore, for the 18 clusters, we reduce the limiting magnitude from 14.3 mag to 13.3 mag to study the effect of stellar crowding. In this case, four clusters have less than 35 members, so they are removed from the test. Some  $\mathcal{R} - N_{\text{top}}$  plots of new clusters are presented in Figure 10. We find the judgements about the mass segregation for the remaining 14 clusters hold. This means that the effect of stellar crowding should not affect our results.

Observationally, the determination of radius always has some uncertainties. To study the effect, we make the radius smaller than the adopted value in Section 4, assuming the uncertainty is 20%. In this case, 16 clusters have more than 35 members. Some of the new  $\mathcal{R} - N_{\text{top}}$  plots are shown in Figure 11. Again, although the details are changed, the judgements about mass segregation hold. This means that the uncertainty of the radius is not likely to affect our results.

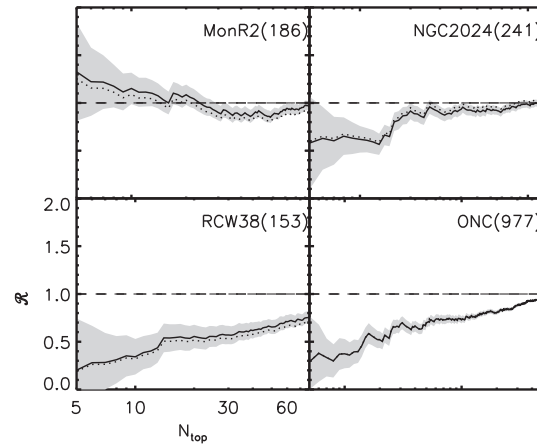


**Fig. 10** The  $\mathcal{R} - N_{\text{top}}$  plot of four clusters. Symbols denote the same as in Fig. 9. The limiting magnitude is set to be 13.3 mag in this test to study the effect of stellar crowding. The dotted line represents the original values.

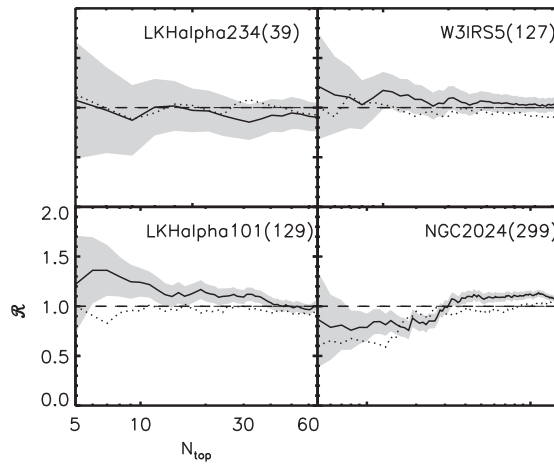


**Fig. 11** The  $\mathcal{R} - N_{\text{top}}$  plot of four clusters. Symbols denote the same as in Fig. 10. In this test, the cluster radii shrink to study the effect of the uncertainty of the radius.

## 5.2 Occurrence of Mass-segregated Clusters and Implications

For the artificial clusters in which the stars are distributed independently of mass, we find 1% of them are level-3 mass-segregated, 27% of them are level-1 mass-segregated, and some of them show inverse mass segregation. We also randomly choose some control regions in the whole sky and assume all the stars inside form a “cluster.” The results are quite similar to that of artificial clusters. These facts suggest that mass segregation observed in embedded clusters cannot always be an accidental phenomenon, especially for level-3 mass segregation. We consider that level-3 mass segregation must be imprinted by the early dynamical evolution or the star formation of embedded clusters.

Another impressive thing is the deficiency of inversely mass-segregated clusters in observation. This might be caused by the rapid dynamical evolution of inversely mass-segregated clusters. In other words, inverse mass segregation is not a stable status for a cluster, which makes it hardly observed. Note that Vesperini et al. (2009) show that initial mass segregation plays an important role in cluster survival. Also note that not every embedded cluster can survive from the state of molecular cloud to open cluster (Adams & Myers 2001; Lada & Lada 2003). From this perspective, as more observations of embedded clusters are taken, inversely mass-segregated clusters might be found.

### 5.3 What Kind of Embedded Cluster is Likely to be Mass-segregated?

We find some clusters are non-mass-segregated. This is not likely to be caused by an inappropriate bias in our process, because some clues about non-mass-segregated clusters are found in the survey of literature (Lada et al. 1991; Carpenter et al. 1997; Herbig & Dahm 2002). So we believe that cases of non-mass-segregated clusters do exist. Then what kind of embedded cluster is likely to be mass-segregated?

We examine the relationship between the existence of mass segregation and the radius of embedded clusters. No correlation is found, which is consistent with Hasan & Hasan (2011). Besides, we find the number of cluster members appears to be related to mass segregation. For these 18 clusters, the average number of members is 175. That of the mass-segregated clusters is 210 and that of the level-3 mass-segregated clusters is 457. So it seems that richer clusters tend to be mass-segregated.

### 5.4 Origin of Mass Segregation

Bonnell & Davies (1998) argue that embedded clusters are too young to show dynamical mass segregation, but some works show that mass segregation can be achieved by rapid dynamical evolution (McMillan et al. 2007; Allison et al. 2009b; Yu et al. 2011). This suggests that we cannot simply deduce the origin of mass segregation of embedded clusters from their age. Then how can we infer its origin? Velocity—mass dependence of a cluster member can provide useful information. Specifically, if a cluster does not show this dependence, the cluster is not dynamically relaxed, and mass segregation in the non-relaxed cluster should be primordial. By using this idea, Chen et al. (2007) and Pang et al. (2010) verify that the mass segregations in NGC 2244, NGC 6530, and NGC 3603 are primordial.

We find that the shape of the  $\mathcal{R} - N_{\text{top}}$  plot can be another method to deduce the origin of mass segregation. The  $\mathcal{R} - N_{\text{top}}$  plot clearly shows two different kinds of mass segregation in observation. Mass segregation can exist in a rather large mass range, such as CepA, RCW 38, and ONC. In this case, the clusters are likely to be dynamically relaxed, so it is likely to be dynamical mass segregation. On the other hand, mass segregation can only exist in the high-mass end of a cluster, such as NGC 2024. This kind of mass segregation seems to suggest that the top most massive stars form by a special mechanism. So it is likely to be primordial mass segregation.

## 6 CONCLUSIONS

In this paper, we introduce a new approach, the  $\mathcal{R} - N_{\text{top}}$  plot, to describe the mass segregation of clusters, and then apply it to eighteen embedded clusters in our Galaxy. The main points of this work are summarized as follows:

- (1) Eleven of the 18 embedded clusters are mass-segregated, seven clusters are non-mass-segregated, and no inversely mass-segregated cluster is found. That is, mass segregation is not a common phenomenon associated with embedded clusters.
- (2) The shape of  $\mathcal{R} - N_{\text{top}}$  plots reveals that there are two kinds of mass segregation, which can give hints about the origin of mass segregation. For a dynamical mass-segregated cluster, its

$\mathcal{R}$  should be lower than unity in a large range. For a primordial mass-segregated cluster, its  $\mathcal{R}$  should only be lower than unity in the high-mass end.

- (3) We find that the richer clusters tend to present mass segregation.
- (4) Absence of inversely mass-segregated clusters suggests that the distribution of stars in embedded clusters is not totally mass-independent.

**Acknowledgements** We are grateful to Richard de Grijs, M. B. N. Kouwenhoven, and Christoph Olczak for their discussions and suggestions. This publication makes use of data products from the Two Micron All Sky Survey, which is a joint project of the University of Massachusetts and the Infrared Processing and Analysis Center/California Institute of Technology, funded by the National Aeronautics and Space Administration and the National Science Foundation. This work is supported by the National Natural Science Foundation of China (Grant Nos. 10873037, 10921063, 10733030 and 10833001).

## References

- Adams, F. C., & Myers, P. C. 2001, *ApJ*, 553, 744  
Allison, R. J., Goodwin, S. P., Parker, R. J., et al. 2009a, *MNRAS*, 395, 1449  
Allison, R. J., Goodwin, S. P., Parker, R. J., et al. 2009b, *ApJ*, 700, 99  
Anderson, J., & King, I. R. 2003, *AJ*, 126, 772  
Ascenso, J., Alves, J., & Lago, M. T. V. T. 2009, *A&A*, 495, 147  
Bonatto, C., & Bica, E. 2003, *A&A*, 405, 525  
Bonatto, C., & Bica, E. 2005, *A&A*, 437, 483  
Bonatto, C., Santos, J. F. C., Jr., & Bica, E. 2006, *A&A*, 445, 567  
Bonnell, I. A., Bate, M. R., Clarke, C. J., & Pringle, J. E. 1997, *MNRAS*, 285, 201  
Bonnell, I. A., Bate, M. R., & Zinnecker, H. 1998, *MNRAS*, 298, 93  
Bonnell, I. A., & Davies, M. B. 1998, *MNRAS*, 295, 691  
Bonnell, I. A., & Bate, M. R. 2005, *MNRAS*, 362, 915  
Brandl, B., Sams, B. J., Bertoldi, F., et al. 1996, *ApJ*, 466, 254  
Carpenter, J. M., Meyer, M. R., Dougados, C., Strom, S. E., & Hillenbrand, L. A. 1997, *AJ*, 114, 198  
Cartwright, A., & Whitworth, A. P. 2004, *MNRAS*, 348, 589  
Chen, L., de Grijs, R., & Zhao, J. L. 2007, *AJ*, 134, 1368  
de Grijs, R., Johnson, R. A., Gilmore, G. F., & Frayn, C. M. 2002, *MNRAS*, 331, 228  
Dutra, C. M., & Bica, E. 2001, *A&A*, 376, 434  
Dutra, C. M., Bica, E., Soares, J., & Barbuy, B. 2003, *A&A*, 400, 533  
Elmegreen, B. G., Efremov, Y., Pudritz, R. E., & Zinnecker, H. 2000, *Protostars and Planets IV*, eds. V. Mannings, A. P. Boss, & S. S. Russell (Book - Tucson: University of Arizona Press), 179  
Er, X.-Y., Jiang, Z.-B., & Fu, Y.-N. 2009, *Chinese Astronomy and Astrophysics*, 33, 139  
Fischer, P., Pryor, C., Murray, S., Mateo, M., & Richtler, T. 1998, *AJ*, 115, 592  
Gouliermis, D., Keller, S. C., Kontizas, M., Kontizas, E., & Bellas-Velidis, I. 2004, *A&A*, 416, 137  
Hasan, P., & Hasan, S. N. 2011, *MNRAS*, 413, 2345  
Herbig, G. H., & Dahm, S. E. 2002, *AJ*, 123, 304  
Hillenbrand, L. A. 1997, *AJ*, 113, 1733  
Hillenbrand, L. A., & Hartmann, L. W. 1998, *ApJ*, 492, 540  
Hunter, D. A., Shaya, E. J., Holtzman, J. A., et al. 1995, *ApJ*, 448, 179  
Jiang, Z., Yao, Y., Yang, J., et al. 2002, *ApJ*, 577, 245  
Kerber, L. O., & Santiago, B. X. 2006, *A&A*, 452, 155  
King, I. 1962, *AJ*, 67, 471  
King, I. R. 1966, *AJ*, 71, 64

- Kontizas, M., Hatzidimitriou, D., Bellas-Velidis, I., et al. 1998, *A&A*, 336, 503
- Lada, C. J., Alves, J., & Lada, E. A. 1996, *AJ*, 111, 1964
- Lada, C. J., & Lada, E. A. 2003, *ARA&A*, 41, 57
- Lada, E. A., Depoy, D. L., Evans, N. J., II, & Gatley, I. 1991, *ApJ*, 371, 171
- Larson, R. B. 1982, *MNRAS*, 200, 159
- Maíz Apellániz, J., & Úbeda, L. 2005, *ApJ*, 629, 873
- McMillan, S. L. W., Vesperini, E., & Portegies Zwart, S. F. 2007, *ApJ*, 655, L45
- Murray, S. D., & Lin, D. N. C. 1996, *ApJ*, 467, 728
- Nürnberg, D. E. A., & Petr-Gotzens, M. G. 2002, *A&A*, 382, 537
- Pang, X., Grebel, E. K., & Altmann, M. 2010, in *IAU Symposium*, 266, *Star Clusters Basic Galactic Building Blocks throughout Time and Space*, eds. R. de Grijs, & J. R. D. Lépine (Cambridge: Cambridge Univ. Press), 24
- Raboud, D., & Mermilliod, J.-C. 1998, *A&A*, 333, 897
- Sagar, R., Miakutin, V. I., Piskunov, A. E., & Dluzhnevskaja, O. B. 1988, *MNRAS*, 234, 831
- Soares, J. B., & Bica, E. 2002, *A&A*, 388, 172
- Vazquez, R. A., Baume, G., Feinstein, A., & Prado, P. 1996, *A&AS*, 116, 75
- Vesperini, E., McMillan, S. L. W., & Portegies Zwart, S. 2009, *ApJ*, 698, 615
- Yu, J., de Grijs, R., & Chen, L. 2011, *ApJ*, 732, 16
- Zhao, J.-L., Chen, L., & Wen, W. 2006, *ChJAA (Chin. J. Astron. Astrophys.)*, 6, 435